Article

Aerosol Optical Properties of Pacaya Volcano Plume Measured with a Portable Sun-Photometer

Pasquale Sellitto [1],*, Letizia Spampinato [2], Giuseppe G. Salerno [2] and Alessandro La Spina [2]

[1] Laboratoire de Météorologie Dynamique, Institut Pierre Simon Laplace, École Normale Supérieure, PSL Research University, École Polytechnique, Université Paris-Saclay, Sorbonne Université, UPMC Université Paris 6, CNRS, 75005 Paris, France

[2] Istituto Nazionale di Geofisica e Vulcanologia, Osservatorio Etneo, I95123 Catania, Italy; letizia.spampinato@ingv.it (L.S.); giuseppe.salerno@ingv.it (G.G.S.); alessandro.laspina@ingv.it (A.L.S.)

* Correspondence: psellitto@lmd.ens.fr; Tel.: +33-1-4432-2731

Abstract: In this paper, Sun-photometer multichannel measurements of aerosol optical depths (AODs) in the visible and near-infrared spectral ranges, and Ångström parameters of the plume issued from the Pacaya volcano, Guatemala, are presented for the first time. These observations, made during a short-term campaign carried out on 29 and 30 January 2011, indicate a diluted (AODs lower than 0.1) volcanic plume composed of small particles (Ångström exponent ∼1.0 on 29 January and ∼1.4 on 30 January). Results are consistent with an ash-free plume. Finally, the impact of the choice of different wavelength pairs for the calculation of the Ångström parameters from the spectral AOD observations is tested and critically discussed.

1. Introduction

Volcanic emissions have important impacts on the atmospheric composition (e.g., [1,2]), cloud distribution (e.g., [3]) and regional (e.g., [4]) to global climate (e.g., [5]). The direct climate forcing of volcanic plumes critically depends on the optical and micro-physical properties of the volcanic aerosols, that in turn depend on the evolution processes of the effluents in the atmosphere [6]. Despite sulphur dioxide (SO2) being only the third most abundant gas species in the volcanic gas mixture (after water vapour and carbon dioxide), it may strongly perturb the atmospheric composition due to its conversion to sub-micron-sized secondary sulphate aerosols (SSA) (e.g., [7]). Over their atmospheric lifetime, SSA particles can undergo condensation, growth and chemical and micro-physical processes when interacting with volcanic ash. All these processes, that are generally scarcely characterised, contribute to determining the radiative properties of volcanic aerosols and hence the direct radiative forcing of volcanic emissions. The micro-physical properties of volcanic aerosols may also play a role in a number of other atmospheric processes, including their interaction with cloud fields (aerosol indirect climatic effect). The net indirect effect of volcanic aerosols is debated [8].

In many cases, micro-physical properties of aerosols are not directly accessible by observations or modelling. Optical proxies of these aerosol properties, for example the aerosol optical depth (AOD) or Ångström exponent (α), are, on the contrary, commonly observed both by satellite and ground-based photometers and spectrophotometers. Therefore, observing the optical properties of volcanic aerosols is crucial to assess their direct and indirect forcing on the atmospheric radiative balance at a number of spatial and temporal scales.

The optical properties of volcanic aerosols can be measured in the near-field, i.e., in proximity and/or in the surrounding area or emitting vents, using portable Sun-photometers such as the Microtops-II. Thanks to their small size and weight, these hand-held instruments are very well suited to field measurement

of volcanic plumes near the source, in difficult access areas. In the past, Microtops-II "Sun Photometer" systems (hereafter referred to as MIISP), have been used to characterise the optical properties of plumes, i.e., to observe the spectral AOD in the visible and near infrared (NIR) spectral ranges, and to derive the Ångström coefficients α and β, from volcanoes such as Mount Etna [9,10], Kilauea [11], Masaya [12], Lascar and Villarica [13,14] and Eyjafjallajökull [15]. Recently, ultraviolet (UV) AOD and UV-to-NIR Ångström coefficient observations have been derived at Mount Etna by means of a Microtops-II "Ozone Monitor" system (hereafter referred to as MIIOM) [16]. These optical properties can be used to gather optical information on the burden and typology (AOD, β) and mean size (α) of the volcanic aerosols and can be used as inputs for dispersion and evolution models that could bridge the near-source characterisation of the plume to the downwind impacts at larger scales (e.g., at the regional scale).

In this paper, near-source observations of the optical properties of the plume of Pacaya volcano (Guatemala) are presented for the first time. Remote MIISP measurements were carried out on 29 and 30 January 2011, during a non-eruptive passive degassing phase. The paper is organised as follows: the MIISP and the methods used in this work to retrieve the optical properties of the plume are introduced in Section 2; the volcanology and visual observations during the campaign are described in Section 3; results are shown and discussed in Section 4; finally, conclusions are given in Section 5.

2. Instruments and Methods

2.1. The Microtops-II "Sun Photometer"

The multichannel hand-held MIISP Sun-photometer used in this work measures direct Sun radiance (2.5° field of view) in five channels centred in the visible (Ch.1: 440.0 ± 1.5 nm, Ch.2: 675.0 ± 1.5 nm, Ch.3: 870.0 ± 0.3 nm), in a water vapour NIR absorption band (Ch.4: 936.0 ± 1.5 nm) and in the NIR spectral window (Ch.5: 1020.0 ± 1.5 nm), with nominal full band width at half maximum (FWHM) of 10.0 ± 1.5 nm [17,18]. The five channels are used to derive AOD spectra. The NIR Ch.4 is also used to derive water vapour vertical content. The instrument used in the present study was pre-calibrated applying a Langley method at Mauna Loa Observatory, Hawaii. The Sun-pointing alignment is performed manually, with the aid of a Sun target window which projects the Sun position with respect of the input optics.

2.2. Observations of Volcanic Plume Optical Properties with Portable Photometry

At each MIISP acquisition, the photometer measures direct Sun radiance at the ground, at the five spectral channels. Using the internal calibration constant and correcting for the Rayleigh absorption, the photometer automatically calculates the AODs at the five nominal wavelengths. Volcanic AOD data are collected in solar occultation mode by viewing the Sun through the plume. The total AOD of the observation will be made up of the aerosol optical depth of the plume AOD_p and the background aerosol optical depth AOD_b. Using quasi-simultaneous observations (within less than 1 h from in-plume observations, see Table 1) of the background atmosphere, e.g., by pointing the instrument towards the Sun in the absence of volcanic plume, the volcanic AOD is then isolated by applying background atmosphere correction for each individual in-plume observation:

$$AOD_p(\lambda) = AOD(\lambda) - AOD_b(\lambda) \tag{1}$$

Practically, we have performed one preliminary background observation session, each day before the in-plume session, and calculated AOD_b. Background atmosphere and in-plume conditions were identified by visual inspection and this identification is subsequently confirmed by the smaller AOD values and variability of the background. We assume that the atmosphere remains relatively homogeneous between background and plume observations and that the clear atmosphere aerosol optical depth in the volume occupied by the plume is negligible with respect to AOD_b.

The uncertainty of individual AOD retrievals with a MIISP, in the atmospheric window channels, has previously been estimated at 0.02, e.g., [19]. Uncertainties in the retrieved AODs mainly arise

from manual Sun-pointing and internal calibration errors. Higher values are expected in spectral regions affected by the absorption of atmospheric gases, such as Ch.4 (sensitive to water vapour absorption) [16]. The standard deviation of the in-plume AOD σ_{AOD_p} is:

$$\sigma_{AOD_p}(\lambda) = \sqrt{\sigma_{AOD}^2 + \frac{\sigma_{AOD^i_b}{}^2}{n}} \tag{2}$$

with n the number of individual background measurements AOD^i_b made to compute the average background. As *n* is in the order of tens to hundreds, the uncertainty content of AOD_p is approximately σ_{AOD}, and then 0.02, as well.

The plume-isolated AOD spectral variability can be modelled using the empirical Ångström law, using the *α* and *β* parameters [20]:

$$AOD_p(\lambda) = \beta_p \lambda^{-\alpha_p} \tag{3}$$

The *α* parameter is the negative spectral slope of the optical depth in log-log scale and is an optical proxy for the mean size of the sampled aerosol particles. Small or negative *α* values are typical of bigger particles, and bigger values, from about 1.0 to approximately 2.5, are typical of smaller particles. The *β* parameter is the modelled AOD value at 1.0 μm and is related to the amount and chemical composition of the aerosol particles. Using Equation (3), the Ångström parameters for each in-plume MIISP acquisition are derived, in this work, using selected wavelength pairs, in the following way:

$$\alpha_p = -\frac{\ln\left[\frac{AOD_p(\lambda_1)}{AOD_p(\lambda_2)}\right]}{\ln\left[\frac{\lambda_1}{\lambda_2}\right]} \tag{4}$$

$$\beta_p = AOD_p(\lambda_1) \cdot \lambda_1^{\alpha_p} \tag{5}$$

The uncertainties of the derived α_p and β_p can be expressed as follows:

$$\sigma_{\alpha_p} = \left(1/\ln\left[\frac{\lambda_1}{\lambda_2}\right]\right) \sqrt{\left(\frac{\sigma_{AOD_p(\lambda_1)}}{AOD_p(\lambda_1)}\right)^2 + \left(\frac{\sigma_{AOD_p(\lambda_2)}}{AOD_p(\lambda_2)}\right)^2} \tag{6}$$

$$\sigma_{\beta_p} = \lambda_1^{\alpha} \sqrt{\sigma_{AOD_p(\lambda_1)}^2 + \left(AOD_p(\lambda_1) \cdot \ln \lambda_1\right)^2 \sigma_{\alpha_p}^2} \tag{7}$$

Considering the moderate values of the observed plume-isolated AODs during our campaign (typically 0.1 at 440 nm and 0.05 at longer wavelengths) and the mentioned uncertainties of about 0.02 for the AOD, using wavelength couples of 440/870 nm and 440/1020 nm, the uncertainties σ_{α_p} and σ_{β_p} are estimated at about 0.50 to 0.65 (*α*) and 0.02 to 0.04 (*β*).

3. Campaign Conditions

Remote photometric observations of the bulk plume's aerosols from Pacaya volcano (geographical position in Figure 1a) were made on 29 and 30 January 2011. Data were collected from two different sites on the WNW flank of the volcano at a mean altitude of 1700 m a.s.l. and 3.5 Km far from the vent (Figure 1b; 14°23′52.80″ N–90°37′51.69″ W, 14°23′30.26″ N–90°38′4.39″ W, respectively). These sites were chosen to locate the Sun behind the plume during the measurements and plume-sun occultation was ensured by manual adjustment of the tripod gears. Atmospheric background (AOD_b) was measured before each measurements in-plume session (AOD) and plume-isolated optical properties (AOD_p) were derived by applying the method described in Section 2. Plume opacity appeared to vary with variable intensity of degassing pulses. Measurements were taken during times when meteorological clouds were absent (Figure 1c). Wind speed and direction for the days of our field campaign were obtained at 700 and 750 mbar (2500 and 3000 m, respectively) from the NOAA (National Oceanic and Atmospheric

Administration, http://www.arl.noaa.gov) real-time environmental applications and display system (READY), running the Global Data Assimilation System (GDAS) reanalysis model. Data show that between the time of sampling (14:00 and 17:30 UTC Table 1), on 29 January 2011, mean wind speed and direction was 6.5 knots and 132° between 700 and 750 mbar. Instead, on 30 January, mean wind speed was 17 knots with a mean wind direction of 250° SW. Therefore, the plume transport direction, reported in Figure 1b, was retrieved according to the meteorological data together with visual observation in field during the sampling. The time intervals and the subdivision in background and in-plume observations for the two days are listed in Table 1. During the collection, the MacKenney cone of Pacaya Volcano [21] (Figure 1), was quietly degassing, producing pulses of plume steam-gas, which dispersed rapidly southwards in the atmosphere downwind. Unlike what was reported by INSIVUMEH (Instituto Nacional de SIsmología, VUlcanología, MEteorología e Hidrología) [22], no anomalous seismic activity was recorded by the geophysical monitoring network on 29 and 30 January. In Figure 1c, a sketch of the plume section intercepted by the MIISP in-plume observations is shown for the measurements taken on 30 January 2011. Considering a 2.5° field of view and a distance of about 3500 m between the sampling site and Pacaya summit, the intercepted circular area has a radius of about 150 m. This area is comparable with the plume's horizontal extension at summit altitude (see Figure 1c), thus assuring that the measured AODs are representative of the whole plume and not only of a subsection.
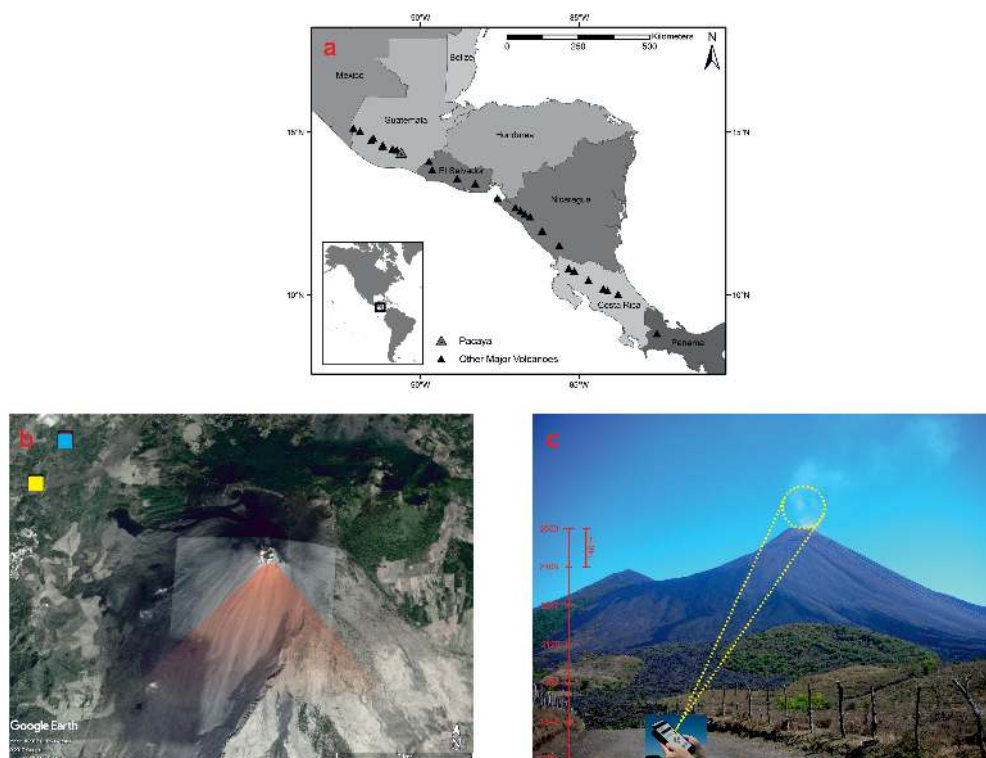

Figure 1. (**a**) Map of the Central American volcanic front [23] showing the location of the volcanoes along the front (black triangles), Pacaya is located in southeastern Guatemala (gray triangle). (**b**) Satellite images of Pacaya showing the direction of plume transport issued by McKenney Cone (reddish area; approximate locations), and the sampling locations from which aerosol optical depth (AOD) measurements were taken on 29 and 30 January 2011 (blue and yellow squares, respectively; Google Earth image CNES 2017). (**c**) View of Pacaya volcano from the western flank of the volcano showing the diluted, roughly vertical plume emitted on 30 January 2011 morning from the volcano summit crater (yellow square in (**b**)). The area of the plume captured by the instrument is also displayed, considering the distance of 3500 m between the sampling site and the summit of Pacaya. The calculated radius of the circular observed area is 150 m above the volcano. The dimension of the plume captured in the photo was scaled considering the altitude of the sampling site and that of Pacaya (1700 and 2550 m, respectively).

Table 1. Dates and time intervals for the background and in-plume observation sessions. All times are UTC.

Day	Type	Time Interval
29 January	Background	15:25–16:00
29 January	In-plume	16:45–17:30
30 January	Background	14:00–14:10
30 January	In-plume	15:10–16:40

4. Results and Discussion

In Figure 2, the AOD observations of Pacaya volcano plume, on 29 and 30 January, at the operating wavelengths of MIISP, are shown. Average values for the background and in-plume sessions are also shown as dotted and solid lines. Observations at 936 nm are excluded due to the water vapour interference in this band. Observations at 675 nm are excluded from the plot to enhance the clarity of the figure: these data points and mean values would have appeared very close to data points for 870 and 1020 nm. As shown in Figure 2, the AOD observations for the in-plume session are systematically larger than the background, at all wavelengths, although both observations are taken at a very small spatio-temporal distance from each other. This suggests that an additional aerosol source is present in the in-plume observations, related to the volcanic source. In addition, the in-plume observations are more variable than the background. While the variability of these latter observations is systematically confined between 0.05 and 0.15, in-plume AOD observations reach values up to 0.6–0.7, depending on the wavelength, indicating an inhomogeneous volcanic aerosol layer.

The spectral variability of average AOD values, for the two days of the campaign, the background, total (in-plume) and plume-isolated observations is shown in Figure 3. For both days, background observations have an almost flat spectral trend, with small variations between shorter and longer wavelengths. This is typical of an atmosphere with an aerosol layer dominated by bigger particles, such as mineral dust or marine aerosols. It should be considered that, although at relatively high altitude, the Pacaya region is only a few tens of kilometres from the Pacific Ocean and thus its background atmosphere could be largely affected by marine aerosols. On the other hand, due to the proximity of this area with Guatemala city (30 km), the impact from anthropogenic pollution, e.g., traffic exhaust emissions, cannot be excluded. The background AODs are larger on 30 January (between 0.10 and 0.12 depending on the wavelength) than 29 January (between 0.05 and 0.07 depending on the wavelength). The total AOD observations are characterised by bigger values than the background, at all wavelengths, thus indicating the presence of an additional aerosol layer (the volcanic plume). The average total AOD reaches values as high as about 0.20 (30 January) and 0.13 (29 January). There is a marked wavelength dependence of the average total AODs, thus indicating that the mentioned additional aerosol layer has smaller particles than the background aerosol layer. The plume-isolated AODs, calculated using Equation (1), are also shown in Figure 2. The marked wavelength dependence is even more apparent than for the total AOD observations, at least at shorter wavelengths. The average plume AOD reaches values as high as about 0.10 (30 January) and 0.07 (29 January) at 440 nm and quickly decreases with wavelength down to values of about 0.05 (30 January) and 0.04 (29 January).

The Ångström parameters α_p and β_p have been subsequently derived using Equations (4) and (5), using different wavelength pairs. Using sufficiently distant wavelengths is crucial to obtain small uncertainties on α_p [16]. Operational MIISP wavelengths in the spectral window region allow multiple choices for the mentioned wavelength pairs, i.e., 440/1020 nm or 440/870 nm. While both combinations are associated to limited uncertainties on α_p, selecting one pair with respect to another is not straightforward. Thus, we have analysed more in-depth the consistency of estimations of the Ångström parameters using these pairs. It has to be mentioned that differences between estimations with different wavelength pairs can be partially attributed to the expected spectral dependency of α_p (and, to a lesser extent, of β_p) (e.g., [24]). The individual α_p and β_p estimations for 29 and 30 January,

using the wavelength pairs 440/1020 nm and 440/870 nm, are shown in Figure 4. The average values of α_p and β_p for both 29 and 30 January are reported in Table 2. The individual α_p estimations vary between about −0.5 and about 2.0, thus indicating the significant inhomogeneity of the plume, with the prevalence of alternatively very big and very small particles. An increase/decrease of over 100% can be observed in extremely short time intervals (e.g., of the order of a few minutes). As an example of this short-term variability, five cases of the occurrence of simultaneous extremely low values of α_p (lower than 0.5) and high values of β (bigger than 0.15) are indicated in Figure 4a. These cases are associated to extreme values of the AOD: 0.20, 0.40, 0.25, 0.50 and 0.20, at 320 nm, and 0.20, 0.45, 0.20, 0.55 and 0.20, at 1020 nm, for the five cases. The simultaneous low values of α and high values of AOD indicate the transitory perturbation of relevant burdens of bigger particles, like for small ash puffs. In any case, mean values of 1.4 ± 0.7 (440/1020 nm) and 1.5 ± 0.9 (440/870 nm), for 29 January, and 1.0 ± 0.5 (440/1020 nm) and 0.8 ± 0.4 (440/870 nm), for 30 January, indicate prevalently small to very small particles, with a significant short-term variability. Similar α mean values have been associated to ash-free plumes in the past, at Mount Etna [9,10,16] and Lascar and Villarica volcanoes [13,14]. The individual β_p estimations vary between near zero to over 0.1. These estimations are inversely correlated with simultaneous α_p estimations. Observations of bigger β and smaller α can be associated with short-term overpasses of ash-bearing plume sections [10,13]. Our results, 0.05 ± 0.07 (440/1020 nm) and 0.05 ± 0.07 (440/870 nm), for 29 January, and 0.03 ± 0.04 (440/1020 nm) and 0.04 ± 0.05 (440/870 nm), for 30 January, denote prevalently ash-free plumes. Nevertheless, it must be mentioned that smaller values of β (0.001 to 0.007) have been observed at Lascar and Villarica volcanoes, while our estimations are more in line with ash-free plumes at, e.g., Mount Etna [9,10].
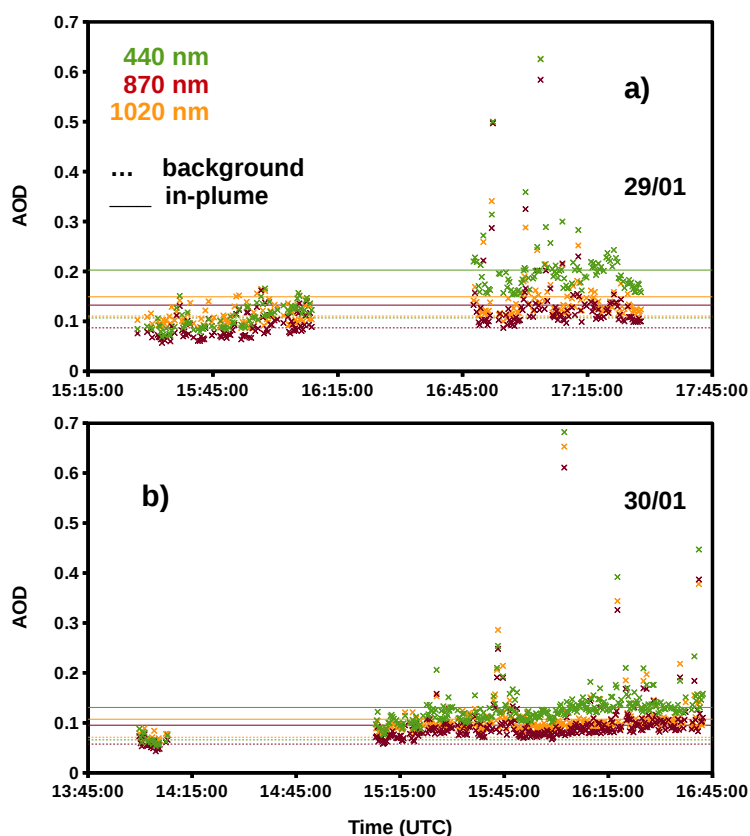

Figure 2. MIISP AOD observations at 440, 870 and 1020 nm on 29 (**a**) and 30 January 2011 (**b**) at Pacaya volcano. Average background (dotted lines) and in-plume AODs (solid lines) are also shown. Background and in-plume measurements are taken during the time intervals of Table 1 (see text for details). All times are UTC.
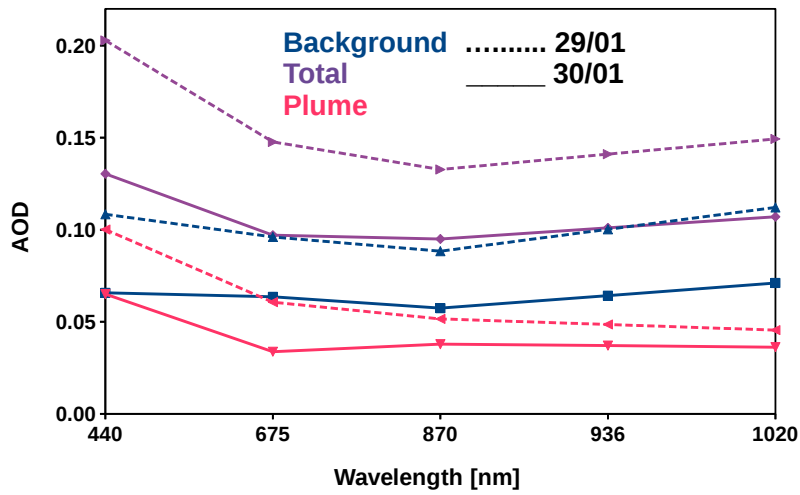
Figure 3. Spectral average MIISP AODs for background (blue symbols and lines) and total atmosphere (violet symbols and lines), and isolated volcanic plume (red symbols and lines), for 29 January (dotted lines) and 30 January (solid lines).
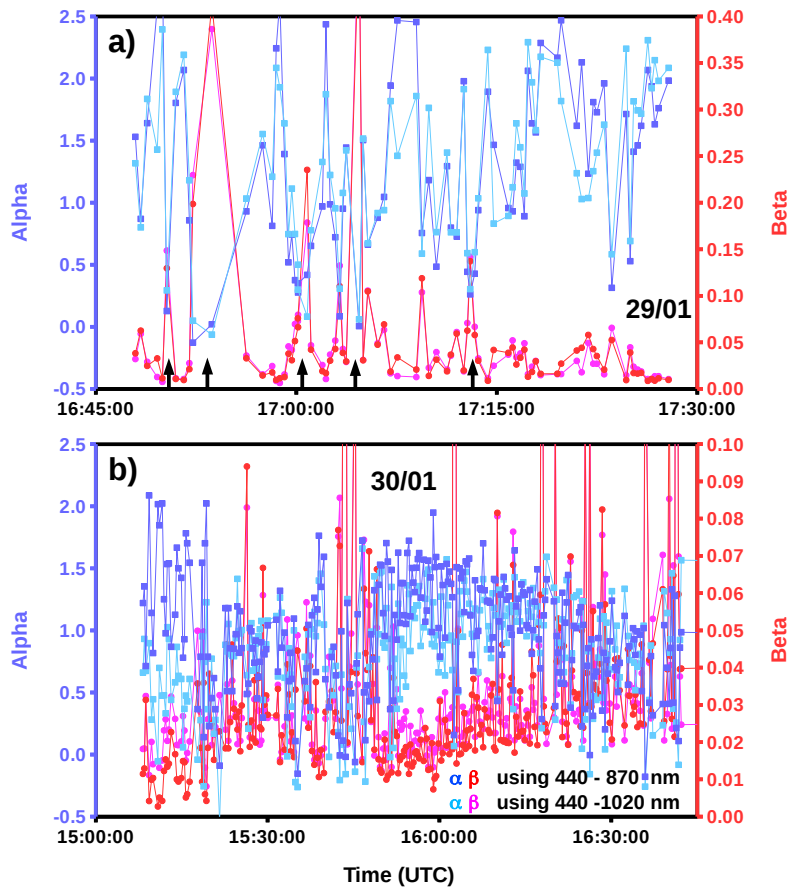

Figure 4. Volcanic plume α_p and β_p observations for 29 January (**a**) and 30 January 2011 (**b**). Determinations with different wavelength pairs are shown, 440/1020 nm (α_p: blue, β_p: red) and 440/870 nm (α_p: sky blue, β_p: pink).

Table 2. Average Ångström coefficients α_p and β_p for the two days of MIISP acquisitions. Average values obtained using different wavelength pairs (440/1020 and 440/870 nm) are reported.

Day	Alpha (440–1020 nm)	Alpha (440–870 nm)	Beta (440–1020 nm)	Beta (440–870 nm)
29 January	1.4 ± 0.7	1.5 ± 0.9	0.05 ± 0.07	0.05 ± 0.07
30 January	1.0 ± 0.5	0.8 ± 0.4	0.03 ± 0.04	0.04 ± 0.05

In the range of our observations, the choice of the wavelength pairs seems not to be a crucial factor in the determination of the mean values of α_p and β_p. The mean values of both parameters, calculated using AODs at 440–1020 nm and 440–870 nm, are well enveloped into each other's statistical uncertainty (measured as 1 standard deviation of the mean, Table 2). In order to obtain more insight into the retrieved data, scatter plots of the individual α_p and β_p measurements, obtained with different wavelength pairs, are shown in Figure 5. In addition, Table 3 shows the Pearson coefficient, root mean square error (RMSE) and mean bias for the four scatter plots. These results reveal that, though a general agreement exists between the mean values of Table 2, the individual observations of α_p can be significantly over/underestimated when using different wavelength pairs. This is the case of of 30 January, with an RMSE of nearly 50%. The β_p determinations, using different wavelength pairs, are more consistent.
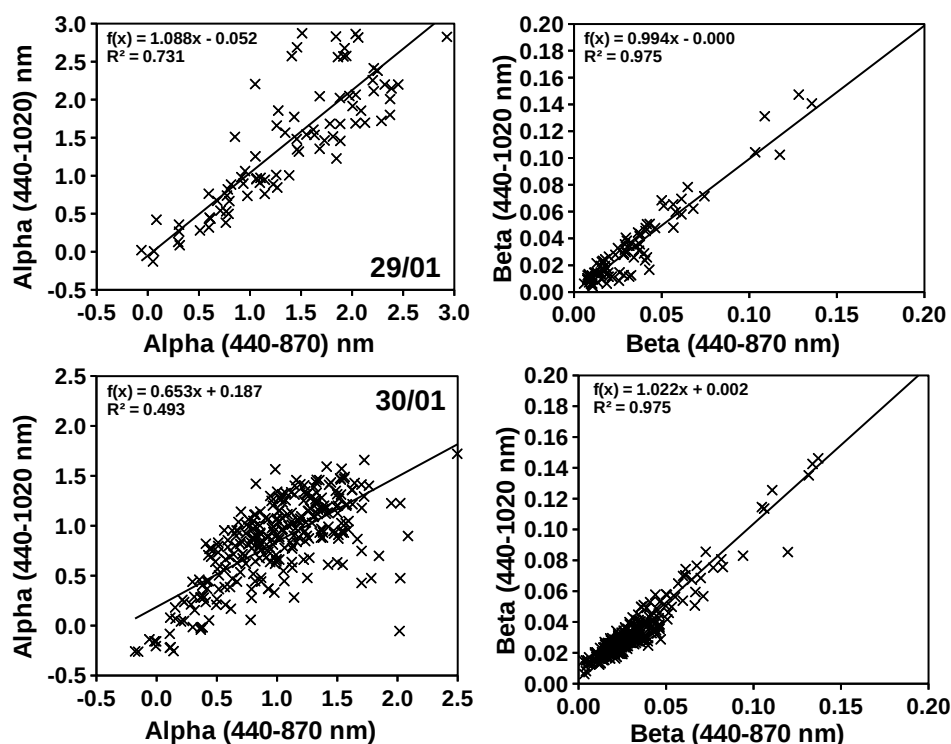

Figure 5. Scatter plots of α_p and β_p measurements with different wavelength pairs, for 29 January (top panels) and 30 January (bottom panels).

Table 3. Statistical parameters for the comparison of α and β with different wavelength pairs (440/1020 nm with respect to 440/870 nm).

	R^2	RMSE	Bias
α—29 January	0.73	28.2%	+14.7%
α—30 January	0.49	47.8%	−17.9%
β—29 January	0.97	25.7%	+6.9%
β—30 January	0.97	22.2%	−2.7%

5. Conclusions

In this paper, the optical characterisation of the volcanic aerosol of Pacaya volcano has been presented. Observations were taken during a field campaign, carried out on 29 and 30 January 2011, using a hand-held MIISP sun-photometer. The volcanic plume was characterised in terms of its spectral AOD in the visible and NIR spectral ranges, and of the subsequently derived Ångström parameters α and β. Overall, moderate plume-isolated AOD values were found. The plume-isolated AOD at 440 nm did not exceed 0.1 during the observation sessions of this campaign. The average α_p (β_p) values of the two measurement sessions are relatively big (small), consistent with an ash-free plume, theoretically composed of a mixture of small secondary aerosols. A potential influence of both marine and anthropogenic aerosol on the aerosol signature of Pacaya region could not be excluded. The use of different wavelength pairs (440–1020 and 440–870 nm) was tested in Ångström parameters retrieval. While the choice of wavelength pairs has a negligible impact on the daily averaged α_p and β_p, individual determinations of these two parameters can be strongly affected by this choice.

Author Contributions: Letizia Spampinato, Alessandro La Spina and Giuseppe G. Salerno conceived, designed and performed the experiments; Pasquale Sellitto analyzed the data; all authors wrote the paper.

Conflicts of Interest: The authors declare no conflict of interest.

References

1. Von Glasow, R.; Bobrowski, N.; Kern, C. The effects of volcanic eruptions on atmospheric chemistry. *Chem. Geol.* **2009**, *263*, 131–142.
2. Sellitto, P.; Zanetel, C.; di Sarra, A.; Salerno, G.; Tapparo, A.; Meloni, D.; Pace, G.; Caltabiano, T.; Briole, P.; Legras, B. The impact of Mount Etna sulfur emissions on the atmospheric composition and aerosol properties in the central Mediterranean: A statistical analysis over the period 2000–2013 based on observations and Lagrangian modelling. *Atmos. Environ.* **2017**, *148*, 77–88.
3. Gassó, S. Satellite observations of the impact of weak volcanic activity on marine clouds. *J. Geophys. Res. Atmos.* **2008**, *113*, D14S19.
4. Sellitto, P.; di Sarra, A.; Corradini, S.; Boichu, M.; Herbin, H.; Dubuisson, P.; Sèze, G.; Meloni, D.; Monteleone, F.; Merucci, L.; et al. Synergistic use of Lagrangian dispersion and radiative transfer modelling with satellite and surface remote sensing measurements for the investigation of volcanic plumes: the Mount Etna eruption of 25–27 October 2013. *Atmos. Chem. Phys.* **2016**, *16*, 6841–6861.
5. Ridley, D.A.; Solomon, S.; Barnes, J.E.; Burlakov, V.D.; Deshler, T.; Dolgii, S.I.; Herber, A.B.; Nagai, T.; Neely, R.R.; Nevzorov, A.V.; et al. Total volcanic stratospheric aerosol optical depths and implications for global climate change. *Geophys. Res. Lett.* **2014**, *41*, 7763–7769.
6. Sellitto, P.; Briole, P. On the radiative forcing of volcanic plumes: modelling the impact of Mount Etna in the Mediterranean. *Ann. Geophys.* **2015**, *58*, doi:10.4401/ag-6879.
7. McCormick, M.P.; Thomason, L.W.; Trepte, C.R. Atmospheric effects of the Mt Pinatubo eruption. *Nature* **1995**, *373*, 399–404.
8. Malavelle, F.F.; Haywood, J.M.; Jones, A.; Gettelman, A.; Clarisse, L.; Bauduin, S.; Allan, R.P.; Karset, I.H.H.; Kristjánsson, J.E.; Oreopoulos, L.; et al. Strong constraints on aerosol-cloud interactions from volcanic eruptions. *Nature* **2017**, *546*, 485–491.
9. Watson, I.M.; Oppenheimer, C. Particle size distributions of Mount Etna's aerosol plume constrained by Sun photometry. *J. Geophys. Res. Atmos.* **2000**, *105*, 9823–9829.
10. Watson, I.M.; Oppenheimer, C. Photometric observations of Mt. Etna's different aerosol plumes. *Atmos. Environ.* **2001**, *35*, 3561–3572.

11. Porter, J.N.; Horton, K.A.; Mouginis-Mark, P.J.; Lienert, B.; Sharma, S.K.; Lau, E.; Sutton, A.J.; Elias, T.; Oppenheimer, C. Sun photometer and lidar measurements of the plume from the Hawaii Kilauea Volcano Pu'u O'o vent: Aerosol flux and SO_2 lifetime. *Geophys. Res. Lett.* **2002**, *29*, 30-1–30-4.

12. Martin, R.S.; Mather, T.A.; Pyle, D.M.; Power, M.; Tsanev, V.I.; Oppenheimer, C.; Allen, A.G.; Horwell, C.J.; Ward, E.P.W. Size distributions of fine silicate and other particles in Masaya's volcanic plume. *J. Geophys. Res. Atmos.* **2009**, *114*, D09217.

13. Mather, T.A.; Tsanev, V.I.; Pyle, D.M.; McGonigle, A.J.S.; Oppenheimer, C.; Allen, A.G. Characterization and evolution of tropospheric plumes from Lascar and Villarrica volcanoes, Chile. *J. Geophys. Res. Atmos.* **2004**, *109*, D21303.

14. Sawyer, G.; Salerno, G.; Blond, J.L.; Martin, R.; Spampinato, L.; Roberts, T.; Mather, T.; Witt, M.; Tsanev, V.; Oppenheimer, C. Gas and aerosol emissions from Villarrica volcano, Chile. *J. Volcanol. Geotherm. Res.* **2011**, *203*, 62–75.

15. Ilyinskaya, E.; Tsanev, V.; Martin, R.; Oppenheimer, C.; Blond, J.L.; Sawyer, G.; Gudmundsson, M. Near-source observations of aerosol size distributions in the eruptive plumes from Eyjafjallajokull volcano, March-April 2010. *Atmos. Environ.* **2011**, *45*, 3210–3216.

16. Sellitto, P.; Salerno, G.; La Spina, A.; Caltabiano, T.; Terray, L.; Gauthier, P.J.; Briole, P. A novel methodology to determine volcanic aerosols optical properties in the UV and NIR and Ångström parameters using Sun photometry. *J. Geophys. Res. Atmos.* **2017**, *122*, 9803–9815.

17. Morys, M.; Mims, F.M.; Anderson, S.E. *MICROTOPS II, Ozone Monitor and Sunphotometer: User's Guide*; Technical Report; Solar Light Company: Glenside, PA, USA, 2001.

18. Morys, M.; Mims, F.M.; Hagerup, S.; Anderson, S.E.; Baker, A.; Kia, J.; Walkup, T. Design, calibration, and performance of MICROTOPS II handheld ozone monitor and Sun photometer. *J. Geophys. Res. Atmos.* **2001**, *106*, 14573–14582.

19. Porter, J.N.; Miller, M.; Pietras, C.; Motell, C. Ship-Based Sun Photometer Measurements Using Microtops Sun Photometers. *J. Atmos. Ocean. Technol.* **2001**, *18*, 765–774.

20. Angström, A. The parameters of atmospheric turbidity. *Tellus* **1964**, *16*, 64–75.

21. Kitamura, S.; Matias, O. *Tephra Stratigraphic Approach to the Eruptive History of Pacaya Volcano, Guatemala*; Seventh Series: Geography 45; Technical Report; Tohoku University: Sendai, Japan, 1995; pp. 1–41.

22. Global Volcanism Program. Report on Pacaya (Guatemala). In *Smithsonian Institution and US Geological Survey Weekly Volcanic Activity Report, 5 January–11 January 2011*; Sennert, S.K., Ed.; Smithsonian Institution and US Geological Survey: Washington, WA, USA, 2011.

23. Carr, M.J.; Rose, W.I., Jr.; Stoiber, R.E. Volcanism in Central America. In *Orogenic Andesites and Related Rocks*; Thorpe, R.S., Ed.; Wiley and Sons: New York, NY, USA, 1982; pp. 149–166.

24. O'Neill, N.T.; Eck, T.F.; Smirnov, A.; Holben, B.N.; Thulasiraman, S. Spectral discrimination of coarse and fine mode optical depth. *J. Geophys. Res. Atmos.* **2003**, *108*, 4559.